Energy-efficient trajectory generation with spline curves considering environmental and dynamic constraints for small UAS

Conference Paper · September 2017

DOI: 10.1109/IROS.2017.8205987

5 authors, including:

Leopoldo Rodriguez Salazar
Universidad de Sevilla
20 PUBLICATIONS **284** CITATIONS
SEE PROFILE

Fotios Balampanis
Universidad de Sevilla
8 PUBLICATIONS **29** CITATIONS
SEE PROFILE

J. A. Cobano
Universidad de Sevilla
40 PUBLICATIONS **458** CITATIONS
SEE PROFILE

Ivan Maza
Universidad de Sevilla
106 PUBLICATIONS **1,824** CITATIONS
SEE PROFILE

Energy-Efficient Trajectory Generation with Spline Curves Considering Environmental and Dynamic Constraints for Small UAS*

L. Rodríguez, F. Balampanis, J. A. Cobano, I. Maza, A. Ollero

Abstract— **This paper presents a method for trajectory generation with Bézier curves, by considering the wind field and dynamic constraints for small Unmanned Aerial Systems (UAS). Atmospheric phenomena affect UAS trajectories, so the wind presence should be considered in order efficiently perform a mission. These missions require precise area decomposition, efficient waypoint sequencing, and a smooth trajectory generation to fulfill the required level of safety and reliability. In this context, a path planning algorithm is presented which incorporates the use of an area decomposition scheme which considers complex shapes and restrictions, in order to provide high levels of coverage. A novel trajectory generation algorithm is proposed, which aims to harvest energy from the atmosphere by taking advantage of the previously estimated wind field and the identified wind features, such as shear wind and discrete gusts, by taking into account flight envelope restrictions. Different test cases and scenarios, including Software-In-The-Loop (SITL) simulations and real telemetry data analysis, are presented to assess the energy gain for the implemented algorithms. The results indicate promising energy gains of almost 15% in voltage saving if the mentioned factors are considered to re-plan the path with the energy-efficient trajectories.**

I. INTRODUCTION

Unmanned Aerial Systems (UAS) operate in the presence of winds, which can affect feasibility, efficiency and optimality of the flight. Therefore, UAS trajectory planning should incorporate the wind effects in order to generate energy-efficient trajectories.

Path planning and trajectory generation for UAS has been extensively studied, mainly focusing on safety and optimality. However, there is a lack of research studies on the UAS trajectory generation considering the wind field as a path designing mean. The wind effects have a relevant role in UAS applications, such as coastal and maritime surveillance, for operations in low altitudes and harsh environments with increased airspace restrictions. In order to perform these operations, an exact area decomposition and an efficient path planning is required. Therefore, these atmospheric effects should be taken into consideration in order to generate a smart path, sequence of waypoints, and energy-efficient trajectories to harvest energy during the flight [1]. This energy can be the result of vertical air motion, spatial wind or temporal gradients.

* This work has been supported by the MarineUAS project (MSCA-ITN-2014-642153), funded by the European Commission under the Horizon 2020 Programme as part of the Marie Sklodowska Curie Actions and by the AEROMAIN project (DPI2014-5983-C2-1-R), funded by the Science and Innovation Ministry of the Spanish Government.

[1] L. Rodriguez, F. Balampanis, J. A. Cobano, I. Maza and A. Ollero are with the Robotics Vision and Control Group (GRVC), University of Seville, (Spain). lrodriguez15, fbalampanis, jcobano, imaza, aollero@us.es

Regarding area decomposition, most of the current approaches in path planning treat a given area either as a continuous space, or as a discrete grid [2]. In both cases, specific area characteristics like non concave complex areas or holes inside the region of interest are not always treated properly [3]. Moreover, there are few studies which take into consideration the on-board sensor for coverage purposes [4]. Complex geographical attributes, task area specificity as also as the need for exact area of interest definition due to airspace restrictions or increased danger mitigation, impose the need for a decomposition which will take into consideration the area properties as well as the UAS and sensor characteristics.

Once the decomposition is performed, a sequence of waypoints that defines a flight plan needs to be designed to fulfill specific requirements that aim to harvest energy from the atmosphere by considering a series of UAS dynamic constraints. An initial requirement is to estimate the wind field and identify wind features [5]. The wind vector estimation has been addressed in many related research efforts [6] [7]. Knowing the wind field, area decomposition replanning can be performed resulting in a new sequence of waypoints, by considering the direction and magnitude of the wind. Furthermore, a more efficient trajectory can be generated even if the sequence is not affected.

The generation of energy-efficient trajectories could be achieved in order to harvest energy from the wind field. This topic has been widely studied in literature; in [8] energy-efficient trajectories are obtained from a dynamic wind field. Also, a method to calculate the shortest Dubins path by considering a known constant wind has been developed in [9]. B-spline curves and Bézier curves has been studied as means to generate smooth energy-efficient trajectories for fixed wing UAS. In [1], the trajectories are generated by optimizing a B-spline curve to perform static and dynamic soaring maneuvers. The previous work is extended by using a GP regression in [10]. Many research efforts utilize B-Spline curves for obstacle-free path generation given a family of discrete optimal paths [11] and planning algorithms based on Bézier curves [12]. In [13] a method which satisfies upper and continuous bounded curvature constraints with a Rapidly-exploring Random Trees (RRTs) algorithm is developed and cubic Bézier curves are utilized to generate continuous curves.

Power consumption should also be considered in this kind of research. In [14], a performance index in a cost function which minimizes the power in soaring maneuvers is used. The exploitation of the wind field for a quad-rotor in urban environments is presented in [15]. A power consumption

model is also used to find minimum-energy trajectories. The work presented in [16] studies the problem formulations for optimal trajectory generation for Micro Air Vehicles (MAVs) in presence of wind, which always results in feasible trajectories despite prevailing wind characteristics.

In literature, the study of the wind field influence in area decomposition replanning and generation of energy-efficient trajectories is not common. The novelty of this paper is to present methods which take into consideration the wind field in two topics: 1) intermediate waypoint addition between two consecutive waypoints of a path generated from a decomposed area; and 2) Smooth trajectory generation and interpolation between two consecutive waypoints, by using detected wind features such as shear wind and discrete gusts.

Regarding the aforementioned literature, this study manages to tackle and improve several aspects:

1) The ground speed and altitude are constant in [15]. This paper estimates the wind field in 3D which influences the flight path generation between a series of waypoints and the corresponding interpolation.
2) Online re-planning considering the estimated wind field. This feature is not considered in [14]–[16].
3) The work presented in [16] considers that the wind speed is constant in different regions, or the magnitude of the wind decreases exponentially. This study considers changes in the wind field in order to improve the path accordingly.

Finally, the proposed methods have been tested by considering different test cases and scenarios, including SITL and the analysis of real telemetry data. The energy gain for the selected methods is also assessed.

II. PROBLEM STATEMENT

The application considered in this paper is coastal and maritime surveillance for operations with UAS in low altitudes as addressed in the MarineUAS European Project (http://marineuas.eu/). The coverage of the area requires an area decomposition in order to obtain an initial path defined by a sequence of waypoints. The used method is based on [17] in which a Constrained Delaunay Triangulation (CDT) [18] is used. The area is segregated in triangular cells and in order to obtain the maximum triangle side constraint of the CDT, an equilateral triangle is inscribed in the Field of View (FoV) projection of the UAS sensor to the sea (see Fig. 1). Note that the projected shape and size are related to the flying altitude as well as the sensor characteristics. Each centroid G of those triangles, serves as a waypoint.

In this paper, the simple case of a camera sensor which is mounted on the UAS is considered. Typically a gimbal is used to maintain the camera pointing down. However, to prevent the weight penalty, this can be imposed as a restriction of the generated path so that the entry points of the curve allow a slope with a low vertical component. Then the platform shall pass through all waypoints in order to gather samples from the whole area. Several costs could be attributed in every waypoint, as described in [17]. For the

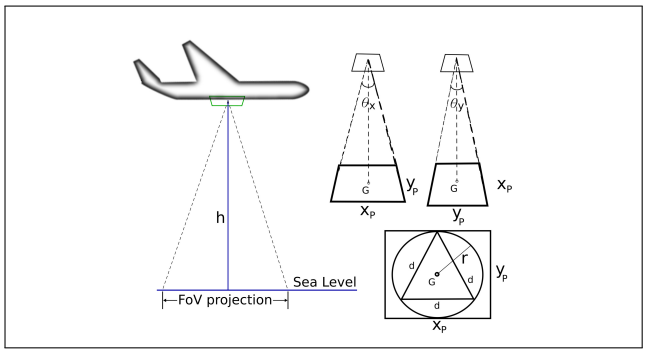

Fig. 1. The Field of View projection of a generic camera sensor to the sea level. It's shape and size are relative to the camera's view angles (θ_x and θ_y), the relative coordinate frames and the altitude h.

purposes of this study, a complete coverage algorithm is used which takes advantage of this triangular cell cost schema.

Finally, a method of finding smooth and energy-efficient trajectories should be implemented. Given a map of the environment, the path given by the area decomposition and the estimated wind field, the algorithm should efficiently compute the energy-efficient trajectory between consecutive waypoints along the complete path, subject to constraints imposed by the UAS capabilities. In order to minimize energy consumption over the trajectory, the cost function, C, is defined as:

$$C = \Delta E_a \tag{1}$$

where ΔE_a is the total energy of the UAS. The following set of constraints are also considered to solve the problem:

- The velocity of the interpolated spline does not have to exceed the maximum turning rate of the platform.
- A number of waypoints has to be selected so that the slope of the curve at the entry and exit of the waypoints has a close-to-zero vertical component. The horizontal component has to balanced between an alignment with the wind predominant direction or with the next waypoint in order to guarantee an energy gain or to prevent an energy loss.

III. ENERGY-EFFICIENT TRAJECTORY

The selected method to generate an energy-efficient trajectory by interpolating a smooth spline, i.e. with continuous curvature at every point, consists in the solution of a tridiagonal system of linear equations, as stated by Hobby in [19]. This application of splines has been widely studied and in general, cubic spline interpolation is commonly proposed [11], [13], [20]. However, dynamic or environmental constraints are not taken into account in typical applications, although there is awareness that the smoothness property favors the control algorithms [1], [21]. Langelaan [7] also proposed the use of splines for characterization of the wind gradient curve as a means to approximate it better, but not in the trajectory generation problem.

The idea of the approach is to parametrize a Bézier curve by determining two of its control points according to specific

parameters optimized for smoothness with the possibility of an energy gain . UAS dynamic constraints are also taken into account.

Let $\hat{m}_i$ be a slope unitary vector so that the slope of the curve at a waypoint, R_i, is determined. In addition, two tension parameters, τ_{in} and τ_{out}, can be defined to modify the rate of decline of the curve. The resultant curve can be parametrized at every waypoint in terms of incoming and outgoing curvature velocity vectors, S_{in} and S_{out} respectively.

A correlation could be established, so that the parameters defining the curvature function of the Bézier spline, bear specific dynamic constraints of the UAS, such as, angle of attack, attitude (particularly important for the footprint in the absence of a gimbal) and other flight envelope parameters, together with the possibility of generating a trajectory that can harvest the atmospheric energy to increase the flight efficiency.

A. Wind Gradient Characterization

In order to generate a soaring-like maneuver, i.e. dive-in/climb, and a direction to maximize the energy gain, a wind field needs to be identified and characterized. For this study, only a shear wind is considered since gusts introduce a complexity on the decision algorithm. Thus, the shear wind can be modeled as a horizontal wind gradient $\frac{dW_x}{dz}$, which can be defined as [1]:

$$W_x = \begin{cases} \beta_{\text{tr}} \left(Az + \frac{1-A}{z_{\text{tr}}} z^2 \right) & 0 \leq z \leq z_{\text{T}} \\ 0 & z < 0 \\ \beta_{\text{tr}} \left(Az_{\text{T}} + \frac{1-A}{z_{\text{tr}}} z_{\text{T}}^2 \right) & z > z_{\text{T}} \end{cases} \tag{2}$$

with the first derivative, defining the gradient, as:

$$\frac{dW_x}{dz} = \begin{cases} \beta_{\text{tr}} A + 2\beta_{\text{tr}} \frac{1-A}{z_{\text{tr}}} z & 0 \leq z \leq z_{\text{T}} \\ 0 & z < 0 \\ 0 & z > z_{\text{T}} \end{cases} \tag{3}$$

where W_x is the total horizontal wind speed, A defines the gradient profile of the altitude, i.e. exponential for $(A < 1)$ or logarithmic for $(1 < A < 2)$, β_{tr} is the wind gradient slope at the characteristic altitude, z_{tr} and z_{T} is the altitude in which the gradient becomes zero.

The predominant wind direction should be identified by analyzing the mean and running standard deviation between estimates of the instantaneous wind vector. A Direct Computation (DC) method [22], [23] is utilized to estimate this vector, by determining the vectorial difference between the ground speed, obtained with the GNSS-aided velocity, $\dot{r}$, and the airspeed, V_a, which can be characterized by using a pitot probe:

$$W = \dot{r} + V_a \tag{4}$$

In general this method is accurate for stable winds; however, different authors [6], [24] consider that the wind is the sum of a stable part and a stochastic process, which can be estimated using an Extended Kalman Filter (EKF) for the Dryden transfer functions in the frequency domain.

In this work, the measurement of the running standard deviation allows to characterize and distinguish between features, by evaluating a series of standard deviation characteristics as stated in [5]. The estimation of the wind vector can also include information from weather reports, such as METAR reports. This information allows a faster computation of the wind gradient and wind direction since the wind characterization algorithm is able to utilize preexisting data [5] by incorporating wind information of weather databases to assess the stability and roughness of a wider area.

The proposed trajectory generation algorithm should perform a new path planning from the flight plan given by the area decomposition method, considering a reported predominant wind in order to generate intermediate waypoints. These waypoints ensure that UAS passes through each waypoint of the initial path to perform the mission as an initial control approximation.

B. Curve Characteristics

A smooth and energy-efficient trajectory should be generated from all the waypoints that defining the path. The curvature smoothness, k, provides an assessment on the desired characteristics of the curve and to determine the Bézier control points. The curvature for a curve, $R(t)$, is given by:

$$k = \frac{||\dot{R}(t) \times \ddot{R}(t)||}{||\dot{R}(t)||^3} \tag{5}$$

The smoothness of the curve is often obtained by integrating the square of (5) over the arc length. The numerical integration of the curve over the arc length is often slow and imprecise [19]. An alternative measure of smoothness consists in determining the maximum value of the change of curvature over the arc length, s, in a given time interval:

$$\max_{0 \leq t \leq 1} \left| \frac{dk}{ds} \right| \tag{6}$$

To determine an acceptable level of smoothness, Hobby [19] states that the velocity vectors, S_{in} and S_{out}, aim to minimize (6). If these velocity functions are fixed for all the waypoints in $R(t)$ the smoothness measures can present local minimums and may produce discontinuities.

The proposed velocity functions are given by:

$$S_{\text{in}}(\xi, \eta) = \frac{2 + a}{1 + (1 - C)\cos\xi + C\cos\eta} \tag{7}$$

$$S_{\text{out}}(\xi, \eta) = \frac{2 - a}{1 + (1 - C)\cos\eta + C\cos\xi} \tag{8}$$

where

$$\xi = \arg\ \hat{g}_i - \arg\ (R_{i+1} - R_i) \tag{9}$$

$$\eta = \arg\ (R_{i+1} - R_i) - \arg\ \hat{g}_{1+1} \tag{10}$$

$$a = A(\sin\xi - B\sin\eta)(\sin\eta - B\sin\xi)(\cos\xi - \cos\eta) \tag{11}$$

The values of the constants A, B and C are chosen to minimize an error function based on the value of the curvature in

(5). A least-squares fit can be used to determine their values, however, this method presents problems for large velocities [19]. Thus, the chosen initial values, which are commonly used for spline generation in computation applications are [19]: $A = \sqrt{2}$, $B, = 1/16$ and $C = \frac{1}{2}(3 - \sqrt{5})$.

In addition, the maximum curvature as a function of time, $k(t)$, can be constrained by the maximum turning rate of the UAS, if a proper tangential velocity can be maintained throughout the curve. The maximum turning rate, ω, can be expressed in terms of the maximum load factor, $n_{\max}$, and the airspeed of the UAS, V_a:

$$\omega_{\max} = \frac{g\sqrt{n_{\max}^2 - 1}}{V^2} \tag{12}$$

$$n_{\max} = \frac{\rho V_a^2 C_{L_{\max}} S}{2mg} \tag{13}$$

where m is the vehicle mass, g is the gravitational constant, ρ corresponds to the air density and $C_{L_{\max}}$ is the maximum lift coefficient.

Therefore, the velocity vector generation function should be reshaped (i.e. changing the constant values) if the maximum curvature exceeds the maximum turning rate.

The slope unitary vector, $\hat{m}_i$, is normally given by the 3D planar direction between two points in $\mathbf{R}^3$. However, for wind field exploitation, the vector can be adjusted to obtain a positive component parallel to the predominant wind direction. Furthermore, this vector can be also aligned ensuring that the m_z component is always zero, so that the UAS passes at the entry and exit point with a very low pitch angle, θ, which is a desired characteristic for maintaining a constant footprint over the waypoints. Additionally, the slope unitary vector should ensure that the maximum angle of the curve does not exceed the maximum angle of attack, $\alpha_{\max}$.

The Bézier control points are four and have to be defined in terms of the velocity functions, tensions and the slope unitary vectors [19]. Note that two of the control points, first and last, correspond to the consecutive waypoints of the path. Considering the dynamic constraints mentioned above, for a spline between two consecutive waypoints, R_i and R_{i+1}, the two remaining control points are defined as:

$$P_0 = R_i \tag{14}$$

$$P_1 = R_i + \frac{\S_{\mathbf{in}}(\xi_i, \eta_{i+1})}{3\tau_i} ||R_{i+1} - R_i|| \hat{m}_i \tag{15}$$

$$P_2 = R_{i+1} \tag{16}$$

$$P_3 = R_{i+1} \frac{\S_{\mathbf{out}}(\xi_i, \eta_{i+1})}{3\tau_{i+1}} ||R_{i+1} - R_i|| \hat{m}_{i+1} \tag{17}$$

The proposed polynomial for a cubic interpolation of the control points is:

$$R(t) = K_3 t^3 + K_2 r^2 + K_1 R_1 + K_0; \tag{18}$$

where the K_n parameters are defined as functions of the control points P_n:

$$K_0 = P_0 \tag{19a}$$

$$K_1 = 3 * (P_1 - P_0) \tag{19b}$$

$$K_2 = 3 * (P_0 - 2P_1 + P_2) \tag{19c}$$

$$K_3 = -P_0 + 3(P_1 - P_2) + P_3 \tag{19d}$$

C. Energy Assessment for Wind Efficient Trajectories

The generated trajectories should ensure an energy gain by using the available energy from the atmosphere. This paper focuses the energy gain on extracting energy from the wind gradient defined in (2) and (3) [1], [14].

First, a no-thrust case is analyzed. This is performed due to the dive-in/climb maneuver which will allow an increase of the kinematic energy, only due to the total wind gradient $\mathbf{J_w}\dot{R}$. The total energy of the UAS, E_a, can be described as the sum of the potential and kinematic energy of the UAS:

$$E_a = -mgz + \frac{1}{2} m V_a^2 \tag{20}$$

Taking the first derivative of (20) over time:

$$\dot{E}_a = -mg(V_a \sin\alpha - W_z) + mV_a \frac{dV_a}{dt} \tag{21}$$

equation (21) can be divided by the mass of the platform to obtain the change of energy per unit of mass. Using the equations of motion for a 6DOF model, which considers the wind gradient for its longitudinal dynamics [1], [25], [26], the rate of change of the energy as a function of the wind gradient, drag (D) and wind velocity (W), can be obtained:

$$\frac{\dot{E}_a}{m} = V_a \frac{D}{m} - gW_z - V_a \begin{bmatrix} \cos\beta_a \cos\alpha_a \\ \sin\beta_a \cos\alpha_a \\ -\sin\alpha_a \end{bmatrix}^{\mathrm{T}} \mathbf{J_w}\dot{R} \tag{22}$$

where β_a is the horizontal angle between the flight path and the wind vector (sideslip), and α_a is the vertical angle between the flight path and the wind vector (angle of attack).

Therefore, the total energy can be obtained by integrating (22) over time. Furthermore, if (22) is positive, there is a positive gain due to the wind gradient, i.e. if the third term of the equation is positive [1].

Given the dynamic constraints and the possibility of wind field consideration, the energy gain cannot be applied to every waypoint in an efficient manner. There might be cases in which, in order to ensure coverage, one has to perform windward or leeward maneuvers over the wind field against the predominant direction. Furthermore, the curvature and continuity property of the path might suffer if the environmental constraints, due to wind, are heeded for every waypoint. Therefore, the proposed solution weights in the horizontal direction of the next waypoint in order to maximize a potential energy gain by assessing the choice of the slope unitary vector and to increase the tension parameters based on the following cases:

$$\begin{cases} \arctan\frac{R_{y_{i+1}}-R_{y_i}}{R_{x_{i+1}}-R_{x_i}} - \arctan\frac{W_y}{W_x} < \frac{\pi}{2} & \hat{m}_i \approx \frac{(W_x,W_y,0)}{||W||} \\ \arctan\frac{R_{y_{i+1}}-R_{y_i}}{R_{x_{i+1}}-R_{x_i}} - \arctan\frac{W_y}{W_x} > \frac{\pi}{2} & \hat{m}_i = \frac{W_{i+1}-W_i}{||W_{i+1}-W_i||} \end{cases} \quad (23)$$

IV. Experimental Results

Several validation tests with real data have been performed to evaluate the implemented algorithms.

A. Software-In-The-Loop Simulations

The first test case consists of a SITL simulation. The area of interest is a coastal region between the Adriatic islands of Otok Plavnik and Cres in Croatia (see Fig. 2).

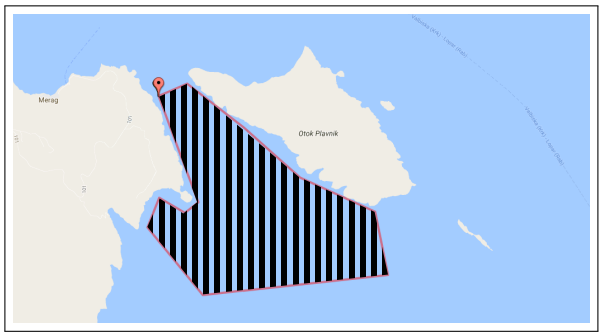

Fig. 2. Area of interest considered in the test cases.

Once the waypoint sequencing algorithm is performed, by using the decomposition and waypoint extraction algorithms proposed in [17] and considering a footprint size of $f =$ 300 m, the resultant waypoint sequence for the UAS can be observed in Fig. 3.

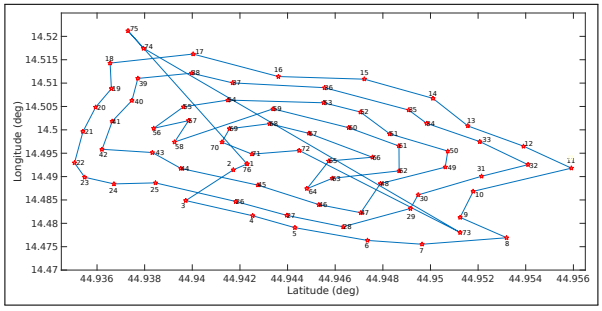

Fig. 3. Sequence of waypoints in the selected area.

Then, the simulation is performed with the JSBSIM library [27] enabled for the Pixhawk [28] SITL Simulator [29] with the Rascal 101 UAV. Table I describes the conditions of the simulated flights.

TABLE I
Selected Flight Cases for SITL Simulation

	Predomintant Wind	Wind Gradient	Splines
Flight 1	$W_x = 0$ m/s	No	No
Flight 2	$W_x = 10$ m/s	No	No
Flight 3	$W_x = 10$ m/s	No	Yes
Flight 4	$W_x = 10$ m/s	Yes	Yes

Note that for Flights 1, 2 and 3 the altitude remains constant on all the waypoints over the flight path. However, slight changes on altitude are performed for the Flight 4 in order to perform dive-in/climb maneuvers that will allow the vehicle to turn off the engine and gain energy.

The first spline interpolation is performed without considering the wind vector. However, the interpolation considers the dynamic constraints of the Rascal UAV which are: a maximum angle of attack of 30º and a maximum turning rate that takes into account a speed limit of 30 m/s. A comparison between the interpolated path and the actual path during the simulation with and without wind are shown in Fig. 4

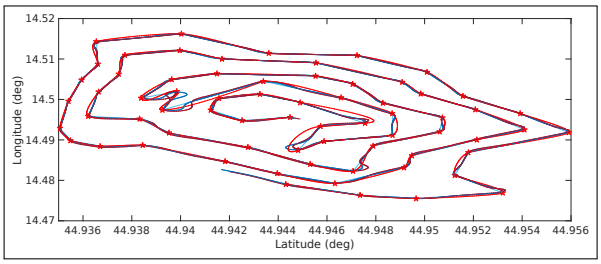

Fig. 4. Comparison between flight path for Flights 1, 2 and 3 (blue line) and the interpolated path (red line).

In Fig. 4 the splines maintain a smooth curvature over the path. By zooming over the area with more waypoint density, one can observe the actual curvature smoothness, even in sharp turns. This can be observed in Fig. 5.

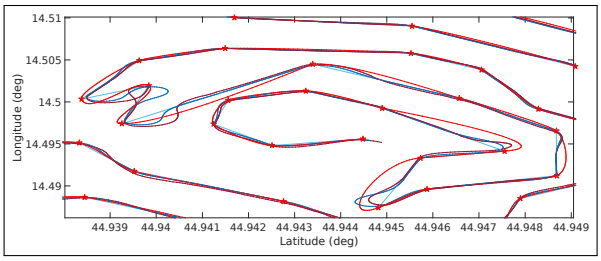

Fig. 5. Sequence of waypoints in the selected area for one UAS.

The computational time of the operation is slightly increased, since the tension parameters and the slope unitary vectors need to be modified for a selected group to keep the curvature at steady levels.

Flight 4 takes into account the full wind field (horizontal wind + gradient over altitude) and path processing has two significant differences; one is that additional waypoints are introduced at lower altitudes between specific waypoints on which UAS can take greater advantage of the wind gradient in the form of an airspeed increase, even if the power plant is off. The other is that some of the waypoints are aligned with the estimated wind field. A detail of the trajectory is presented in Fig.6, in which these two conditions are shown.

The results of the SITL simulations are presented comparing the distance between the waypoints, the flight time duration, the maximum airspeed and the difference between the start and final voltage (see Table II).

It can be observed that for Flight 2, the energy consumption (voltage measurement) is the highest among the four

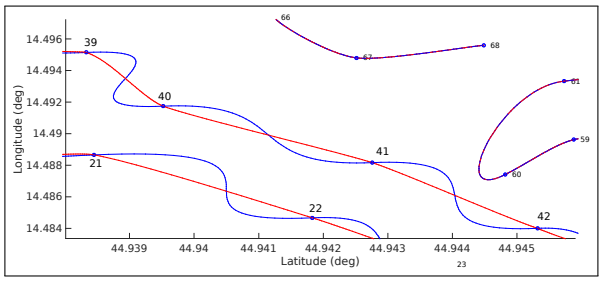

Fig. 6. Spline generation considering the wind field for slope unitary vector (blue) and trajectory without considering the wind field (red).

TABLE II

SITL SIMULATION RESULTS IN TEST CASES.

Flight	Dist (m).	Time (min)	$V_{a_{\max}}(m/s)$	V_0	V_f
1	25536	21.38	21.20	12.4	6.43
2	25936	21.61	20.63	12.4	6.09
3	25229	21.02	21.14	12.4	6.36
4	25301	21.20	25.9	12.4	7.18

cases. This case considers the simulated north wind. Note that there is a significant number of times where the UAS flies towards the wind, which produces an increase on the drag and the requirement of more power (see Fig. 4). Then, Flights 1 and 3 have similar energy results and the duration of the time is considered. This shows that the proposed trajectory with splines prevents a voltage penalty even if the wind is not considered. Finally, Flight 4 has a significant voltage saving, because the places in which the aircraft is flying towards the wind, it performs a series of engine-off dive-in/climb maneuvers which allow an increase of airspeed (up to 40%) with no voltage penalty associated.

B. Comparison between SITL and real-life experiment

This analysis compares two real flights, performed in the region of Agdenes in Norway with the Skywalker X8 UAV (see Fig. 7), against a SITL simulation in the same area. The SITL simulation considers the characteristics of the Skywalker X8 FPV [30] and the aerodynamic coefficient estimations following the method presented in [6].

Fig. 7. The Skywalker UAS utilized in the flights in the region of Agdenes Norway

The voltage of the first flight, compared to the theoretical voltage that can be obtained during the spiral maneuvers, if the splines are optimized and the engine is off, is shown in Fig. 10.

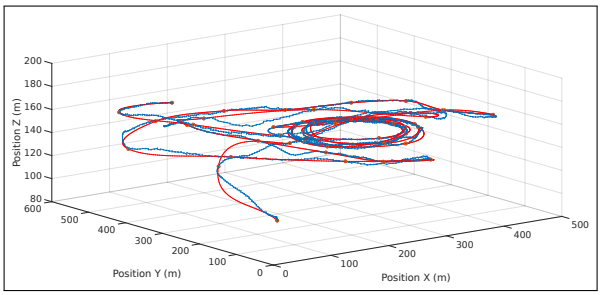

Fig. 8. UAV Trajectory for second flight (blue) and spline interpolation (red) considering waypoint vectorial difference as slope unitary vector.

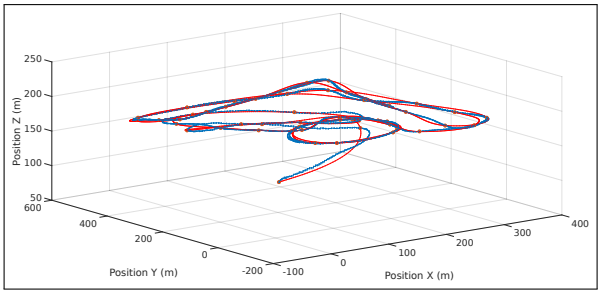

Fig. 9. UAV Trajectory for second flight (blue) and spline interpolation (red) considering waypoint vectorial difference as slope unitary vector.

Table III shows the comparison between the real and simulated data.

TABLE III

SITL SIMULATION RESULTS COMPARED.

Flight	Dist (m).	Time (min)	V_0	V_f
1	6923	5.76	16.56	14.33
2	7128	6.01	16.51	14.21
1_{SITL}	6629	5.52	16.56	15.48
1_{SITL}	6947	5.78	16.51	15.16

V. CONCLUSIONS AND FUTURE WORK

The results show that the performance of the proposed interpolation method fulfills the requirements, providing the UAS with an energy gain, in the form of voltage saving, of almost 15% if the wind field is considered and the dynamic constraints are imposed for the spline generation. The main contribution is that the curve parametrization considers specific characteristics of the UAS and the environment,

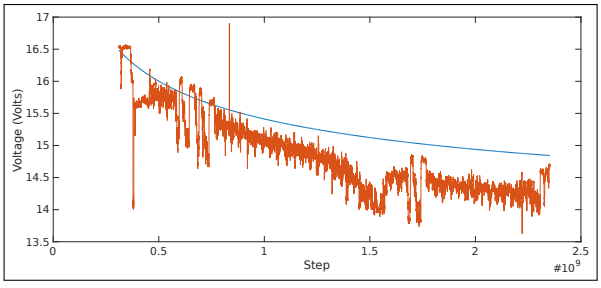

Fig. 10. Real voltage drop on first flight, and SITL voltage drop considering the interpolated splines.

the estimated wind field and identified wind features; this occurs not only as constraints but also as design parameters for the position of the control points and in consequence for the curvature. For the SITL simulations, the two flights which consider the interpolation tend to minimize flight time, flight distance and also maximize energy efficiency. In order to validate the results, two additional cases were presented in which two SITL simulations are compared with two experiments performed in Agnedes-Norway, showing that the method for interpolation produces flyable paths. Furthermore, the novel trajectory generation method is able to modify specific curve parameters both on a waypoint-to-waypoint basis and on a flight path basis in order to keep the trajectories flyable and avoid discontinuities or drastic curvature changes.

Future work includes the design of a trajectory tracking system in order to maximize the energy gain. Up to this point the controllers are considered slow and by designing a proper controller will allow more aggressive soaring maneuvers which will impose less stringent restrictions for the trajectory design. In addition, a full validation and verification stage with the real-time on board implementation of the trajectory path generation algorithm is planned.

ACKNOWLEDGMENT

The authors want to thank Andreas Wenz and Prof. Tor Arne Johansen from the NTNU AMOS - Centre for Autonomous Marine Operations and Systems, for assisting this research by providing experimental data from their testing campaign in Agdenes Norway in order to perform the validation of our methods.

REFERENCES

[1] C. Gao, "Autonomous soaring and surveillance in wind fields with an unmanned aerial vehicle," Ph.D. dissertation, Graduate Department of Aerospace Science and Engineering, University of Toronto, Toronto, Canada, 2015. [Online]. Available: https://goo.gl/IDe5i3

[2] E. Galceran and M. Carreras, "A survey on coverage path planning for robotics," *Robotics and Autonomous Systems*, vol. 61, no. 12, pp. 1258–1276, 2013. [Online]. Available: http://dx.doi.org/10.1016/j.robot.2013.09.004

[3] F. Balampanis, I. Maza, and A. Ollero, "Area Partition for Coastal Regions with Multiple UAS," *Journal of Intelligent & Robotic Systems*, pp. 1–16, 2017.

[4] Y. Li, H. Chen, M. Joo Er, and X. Wang, "Coverage path planning for UAVs based on enhanced exact cellular decomposition method," *Mechatronics*, vol. 21, no. 5, pp. 876–885, 2011.

[5] L. Rodriguez, J. A. Cobano, and A. Ollero, "Small uas-based wind feature identification system part 1: Integration and validation," *Sensors*, 2017.

[6] A. Wenz, T. A. Johansen, and A. Cristofaro, "Combining model-free and model based angle of attack estimation for small fixed-wing uavs using a standard sensor suite," in *2016 International Conference on Unmanned Aircraft Systems (ICUAS)*, June 7-10, 2016, Arlington, VA USA., pp. 624–632.

[7] J. Langelaan, J. Spletzer, C. Montella, and J. Grendestedt, "Wind field estimation for autonomous dynamic soaring," in *2012 IEEE International Conference on Robotics and Automation*, May 14-18, 2012, Saint Paul, MN USA., pp. 16–22.

[8] G. C. Bower, T. C. Flanzer, and A. D. Naiman, "Dynamic environment mapping for autonomous thermal soaring," in *AIAA Guidance, Navigation and Control Conference and Exhibit*, August 02-05 2010, Toronto, Canada.

[9] T. McGee and J. K. Hedrick, "Path planning and control for multiple point surveillance by an unmanned aircraft in wind," in *Proceedings of the 2006 American Control Conference*, June14-16, 2012, Minneapolis, MN USA., pp. 4261–4266.

[10] W. Shaw-Cortez and E. Frew, "Efficient trajectory development for small unmanned aircraft dynamic soaring applications," *Journal of Guidance, Control and Dynamics*, vol. 38, no. 3:2013, March 2015.

[11] D. Jung and P. Tsiotras, "On-line path generation for small unmanned aerial vehicles using b-spline path templates," in *AIAA Guidance, Navigation and Control Conference and Exhibit*, August 18-21 2008, Honolulu, HI USA.

[12] J. Choi and H. Elkaim, "Bézier curve for trajectory guidance," *Autonomous Systems Lab, Computer Engineerin Department, University of California, Santa Cruz*, 2008.

[13] K. Yang and S. Sukkarieh, "3d smooth pat planning for a uav in cluttered natural environments," in *AIAA Guidance, Navigation and Control Conference and Exhibit*, August 18-21 2008, Honolulu, HI USA.

[14] N. Akhtar, J. F. Whidborne, and A. K. Cooke, "Real-time trajectory generation technique for dynamic soaring uav," *Cranfield University*, 2008.

[15] J. ware and N. Roy, "An analysis of wind field estimation and exploitation for quadrotor flight in the urban canopy layer," in *Proceeding of the IEEE International Conference on Robotics and Automation (ICRA)*, May 16-21 2016, Stockholm, Sweden.

[16] Y. Ketema and Y. J. Zhao, "Travel trajectory planning for micro air vehicles in winds," in *AIAA Guidance, Navigation and Control Conference*, August 10-13 2016, Chicago, IL, USA.

[17] F. Balampanis, I. Maza, and A. Ollero, "Coastal Areas Division and Coverage with Multiple UAVs for Remote Sensing," *Sensors*, vol. 17, no. 4, p. 808, 2017.

[18] J. R. Shewchuk, "Delaunay refinement algorithms for triangular mesh generation," *Computational Geometry*, vol. 22, no. 1-3, pp. 21–74, 2002. [Online]. Available: http://www.sciencedirect.com/science/article/pii/S0925772101000475

[19] J. D. Hobby, "Smooth, easy to compute interpolating splines," Department of Computer Science Stanford University, Tech. Rep. STAN-CS-85-1047, 1985. [Online]. Available: https://goo.gl/9wQPwO

[20] L. Fowler and J. Rogers, "Bézier curve path planning for parafoil terminal guidance," *Journal of Aerospace Information Systems*, vol. 15, no. 5, May 2014.

[21] N. T. Depenbusch, "Atmospheric energy harvesting for smal uninhabited aircraft by goost soaring," Pennsylvania, USA, 2011.

[22] J. Langelaan, "Biologically inspired flight tecniques for small and mirco unmanned aerial vehicles," *Guidance, Navigation and Control Conference*, no. 2008-6511, 2008, american Institute of Aeronautics and Astronautics.

[23] L. Rodriguez, J. A. Cobano, and A. Ollero, "Wind field estimation and identification having shear wind and discrete gust features with a small uas," *2016 IEEE/RSJ International Conference on Intelligent Robots and Systems (IROS)*, October 9-14, 2016.

[24] R. W. Beard and T. W. McLain, *Small Unmanned Aircraft: Theory and Practice*. Princenton University Press, February 2012, ch. 4, pp. 54–56.

[25] N. R. J. Lawrance and S. Sukkarieh, "Path planning for autonomous soaring fliht in dynamic wind fields," in *2011 IEEE International Conference on Robotics and Automation*, May 9-13, 2011, Shanghai, China., pp. 2499–2505.

[26] N. R. J. L. an J. J. Acevedo, J. J. chung, J. L. Nguyen, D. Wilson, and S. Sukkarieh, "Long endurance autonomous flight for unmanned aerial vehicles," *Journal AerospaceLab*, no. 8, December 2014.

[27] "Jsbsim, the open source flight dynamics model in c++," http://jsbsim.sourceforge.net/, 2016.

[28] L. Meier, D. Honegger, and M. Pollefeys, "PX4: A node-based multithreaded open source robotics framework for deeply embedded platforms," in *Robotics and Automation (ICRA), 2015 IEEE International Conference on*, may 2015.

[29] "Fixed wing ardupilot instance for autopilot hardware," http://ardupilot.org/plane/index.html, 2016.

[30] "Skywalker x-8 fpv," https://goo.gl/vdDqOh, 2016.